ENERGY PARTITIONING AND ATTENUATION OF GUIDED WAVES IN A RADIALLY LAYERED BOREHOLE

by

D.R. Burns, C.H. Cheng, and M.N. Toksöz

Earth Resources Laboratory
Department of Earth, Atmospheric, and Planetary Sciences
Massachusetts Institute of Technology
Cambridge, MA 02139

ABSTRACT

Recently published results (Tubman et al., 1984; Baker, 1984) indicate that synthetic full waveform acoustic logs generated in cased or damaged boreholes differ significantly from those generated in an open hole with the same formation parameters. In particular, the guided waves appear to be the most affected by such radial layering. In order to gain some understanding of these effects, the amplitude response and energy distribution of the pseudo-Rayleigh and Stoneley waves are studied for the cased and invaded borehole models. The expressions derived by Cheng et al. (1982) are used to calculate partition coefficients (partial derivatives of phase velocity with respect to body wave velocities) for the guided wave modes. The attenuation of the guided wave can then be represented by the sum of the layer attenuation values weighted by their respective partition coefficients. The results indicate that the attenuation of the Stoneley wave is dominated by the fluid attenuation at all frequencies in fast formations, both in the open hole geometry and in the presence of casing or invaded zones. In a slow formation, the Stoneley wave attenuation becomes more sensitive to the shear wave attenuation of the formation at higher frequencies in both the open and cased hole situations. For the pseudo-Rayleigh wave, the introduction of casing reduces the effect of the fluid attenuation, while the presence of an invaded zone reduces the effect of the formation shear attenuation. Plots of the partition coefficients indicate that the casing and invasion layers are most important over a limited frequency range which is related to the thickness of the layer. Radial displacement curves illustrate the depth of penetration of the various frequency components of the pseudo-Rayleigh wave.

INTRODUCTION

Recent interest in the field acquisition of Full Waveform Acoustic Logs (FWALs) has resulted in many studies of wave propagation in a cylindrical borehole (Cheng and Toksöz, 1981; Tsang and Rader, 1979; Paillet and White, 1982). The majority of these have addressed the simple case of a homogeneous, isotropic, infinite solid surrounding a fluid filled cylindrical borehole. Several recent papers (Tubman et al., 1984; Baker, 1984; Chan and Tsang, 1983; Shoenberg et al., 1981) have addressed the more complex problem of solid radial layers surrounding a fluid filled borehole. The common occurrence of drilling induced formation damage or the presence of steel casing and associated cement justify the need to treat this more complicated geometry. The results of Tubman et al. (1984) indicate that synthetic FWALs generated in cased or damaged boreholes can differ significantly from those

generated in an open hole with the same formation parameters. In particular, the guided wave modes, the pseudo-Rayleigh and Stoneley waves, appear to be most affected. When casing and cement are inserted into a borehole the radius of the fluid filled cylinder is decreased. This decrease shifts the pseudo-Rayleigh wave dispersion curves to higher frequencies which, for a constant bandlimited source, results in less excitation and a decrease in amplitude (Cheng and Toksöz, 1981). The Stoneley wave amplitude increases in the same situation due to both the casing providing a more efficient waveguide and the receiver being located closer to the fluid-solid interface where the amplitude is at a maximum. The effects of damaged or invaded zones in the formation are more subtle. Tubman (1984) modelled such zones as a constant radial thickness layer with velocity and attenuation (Q^{-1}) values different from the virgin formation. His results showed a range of waveform effects depending on the thickness and degree of alteration of the zone. The amplitude variations of the pseudo-Rayleigh and Stoneley waves were much less dramatic than the casing examples. Since the borehole size remains constant in the damaged/invaded borehole models, any changes in the amplitudes of the guided waves must be related to the layer parameters of the model. The amplitude varlations for the casing models, however, are due to a combination of borehole size and layer parameters.

In order to gain a better understanding of the effects of the layer parameters the amplitude response and energy distribution of the pseudo-Rayleigh and Stoneley waves will be studied. Cheng et al. (1982) used the variational principle to analytically derive the partition coefficients (partial derivatives of phase velocity with respect to body wave velocity) for any guided wave mode. The attenuation of the guided wave can then be represented by the sum of the layer attenuation values weighted by their respective partition coefficients. The partition coefficients are therefore a measure of the partitioning of the energy of the wave within the layers through which it propagates (Anderson and Archambeau, 1964). It should also be noted that the partial derivatives of the phase velocity with respect to layer parameters are used as a basic tool for interpreting dispersion curves for guided waves in any layered medium. By deriving expressions for these derivatives, the effect of perturbations of layer parameters on the phase velocity dispersion curves of the guided wave can be calculated, resulting in an efficient means of fitting a layered model to the observed data. Cheng et al. (1982) applied this technique to the simple borehole model and used the results to estimate the shear attenuation of the formation. In this paper their results, together with the dispersion equation for a layered borehole as derived by Tubman et al. (1984), are applied to the cased and damaged/invaded borehole models to calculate displacements, partition coefficients, and Stoneley wave attenuation (Q_{st}^{-1}) and pseudo-Rayleigh wave attenuation (Q_{pr}^{-1}). The comparison of guided wave attenuation factors for both the simple borehole and layered borehole models will give an indication of the effect of the layers on the wave amplitudes. Plots of the partition coefficients versus frequency illustrate the frequency range at which different layers have the largest effect on the waveform.

THEORY

Partition Coefficients

A common measure of attenuation is the quality factor, Q, or its inverse, Q^{-1}, the dissipation factor. The dissipation factor can be defined as:

$$Q^{-1} = \frac{\Delta E}{2\pi E} \tag{1}$$

where : ΔE = *strain energy dissipated per stress cycle*

E = *total strain energy stored per cycle*

For a layered medium the dissipation factor for a guided wave can be defined by a summation over all layers (n=1,N) (Anderson and Archambeau, 1964):

$$Q^{-1} = \sum_{n=1}^{N} \frac{E_n}{E} Q_n{}^{-1} \tag{2}$$

The total attenuation for a layered medium can therefore be represented by a summation of the attenuation factors for each layer weighted by the fractional strain energy stored in that layer. For small values of Q^{-1} the attenuation of a guided wave can be written (Anderson and Archambeau, 1964; Aki and Richards, 1980):

$$Q^{-1} = \sum_{n=1}^{N} \frac{\alpha_n}{c} \frac{\partial c}{\partial \alpha_n} Q_{\alpha_n}{}^{-1} + \sum_{n=1}^{N} \frac{\beta_n}{c} \frac{\partial c}{\partial \beta_n} Q_{\beta_n}{}^{-1} \tag{3}$$

where: N = *number of layers*

α,β = *body wave velocities*

c = *phase velocity*

Q_α, Q_β = *body wave attenuation factors*

The coefficients of the body wave attenuation values are referred to as partition coefficients since they are a measure of strain energy partitioning.

For a fluid-filled cylindrical borehole in an isotropic, homogeneous, infinite solid, Cheng et al. (1982) derived an expression for the attenuation of a guided wave:

$$Q^{-1} = \frac{1}{\omega^2 I}\left\{\int_0^\infty \left[\frac{\partial u_r}{\partial r} + \frac{u_r}{r} - k u_z\right]^2 \left(\lambda + 2\mu\right) Q_\alpha^{-1}\, r\,dr \right. \tag{4}$$

$$\left. + \int_0^\infty \left[\left[\frac{\partial u_r}{\partial r}\right]^2 + \left[\frac{u_r}{r}\right] + k^2 u_z^2 - \left[\frac{\partial u_r}{\partial r} + \frac{u_r}{r} - k u_z\right]^2 + \left[k u_r + \frac{\partial u_z}{\partial r}\right]^2\right] \mu\, Q_\beta^{-1}\, r\,dr \right\}$$

$$where: \quad I = \int_0^\infty \rho\left[u_r^2 + u_z^2\right] r dr$$

u_r, u_z = *radial* and *axial displacements*

k = *axial wavenumber*

ω = *angular frequency*

λ, μ = *Lame's constants*

ρ = *density*

They also derived an expression for the partial derivative of phase velocity with respect to density :

$$\frac{\partial c}{\partial \rho} = \frac{-c}{4I} \int_0^\infty \left[u_r^2 + u_z^2\right] r dr \tag{5}$$

Although these expressions were derived for a simple borehole model they can be directly applied to a radially layered borehole by simply evaluating the integrals over specific layers. It should be noted that the derivations of Cheng et al. (1982) were for constant wavenumber (k) which yields expressions for temporal Q^{-1}. To obtain spatial Q^{-1} (which is what could be measured from FWALs) the following relation can be used (Aki and Richards, 1980):

$$Q^{-1}_{spatial} = \frac{c}{U} Q^{-1}_{temporal} \tag{6}$$

$where: U$ = *group velocity*

LAYERED BOREHOLE

In order to evaluate the integrals in equation 6 for a layered borehole, expressions for the displacements and their derivatives are needed. In addition, the dispersion equation for the layered borehole model must be derived to locate appropriate (k,c) pairs for the propagating modes. The axisymmetric wave equation in cylindrical coordinates is:

$$\frac{\partial^2 \varphi_n}{\partial r^2} + \frac{1}{r}\frac{\partial \varphi_n}{\partial r} + \frac{\partial^2 \varphi_n}{\partial z^2} = \frac{1}{\alpha_n^2}\frac{\partial^2 \varphi_n}{\partial t^2} \tag{7}$$

$$\frac{\partial^2 \psi_n}{\partial r^2} + \frac{1}{r}\frac{\partial \psi_n}{\partial r} - \frac{\psi_n}{r^2} + \frac{\partial^2 \psi_n}{\partial z^2} = \frac{1}{\beta_n^2}\frac{\partial^2 \psi_n}{\partial t^2}$$

where: φ_n = *scalar potential*

ψ_n = *azimuthal component of the vector potential*

The solutions are:

$$\varphi_n = [A_n K_0(l_n r) + A_n^1 I_0(l_n r)]\, e^{i(kz-\omega t)} \tag{8}$$

$$\psi_n = [B_n K_1(m_n r) + B_n^1 I_1(m_n r)]\, e^{i(kz-\omega t)}$$

where: $$l_n = k\left(1 - \frac{c^2}{\alpha_n^2}\right)$$

$$m_n = k\left(1 - \frac{c^2}{\beta_n^2}\right)$$

A_n, B_n = *amplitudes of outgoing waves*

A_n^1, B_n^1 = *amplitudes of incoming waves*

$I_i = i^{th}$ *order modified Bessel function of the first kind*

$K_i = i^{th}$ *order modified Bessel function of the second kind*

Displacements in terms of potentials are:

$$u_{r_n} = \frac{\partial \varphi_n}{\partial r} - \frac{\partial \psi_n}{\partial z} \tag{9}$$

$$u_{z_n} = \frac{\partial \psi_n}{\partial r} + \frac{\psi}{r} + \frac{\partial \varphi_n}{\partial z}$$

The expressions for the displacements are therefore (ignoring exponential terms):

$$u_{r_n} = -l_n K_1(l_n r) A_n + l_n I_1(l_n r) A_n^1 - k K_1(m_n r) i B_n - k I_1(m_n r) i B_n^1 \tag{10}$$

$$iu_{z_n} = kK_0(l_n r)A_n + kI_0(l_n r)A_n^1 + m_n K_0(m_n r)iB_n - m_n I_0(m_n r)iB_n^1$$

The radial derivatives of the displacements are:

$$\frac{\partial u_{r_n}}{\partial r} = [l_n^2 K_0(l_n r) + \frac{l_n}{r}K_1(l_n r)]A_n + [l_n^2 I_0(l_n r) - \frac{l_n}{r}I_1(l_n r)]A_n^1 + \quad (11)$$

$$[km_n K_0(m_n r) + \frac{k}{r}K_{1(m_n}r)]iB_i - [km_n I_0(m_n r) - \frac{k}{r}I_1(m_n r)]iB_n^1$$

$$-i\frac{\partial u_{z_n}}{\partial r} = -kl_n K_1(l_n r)A_n + kl_n I_1(l_n r)A_n^1 - m_n^2 K_1(m_n r)iB_n - m_n^2 I_1(m_n r)iB_n^1$$

The dispersion equation for a layered borehole was derived by Tubman et al. (1984) by using a Thomson - Haskell type propagator matrix. The borehole geometry used in their derivation is illustrated in Figure 1. The outer radius of layer n is defined as r_n. Equation (11), together with expressions for normal and tangential stress, can be combined into a motion-stress vector of the form:

$$\mathbf{U}_n = \mathbf{D}_n(r)\,\mathbf{a}_n \quad (12)$$

$$where: \quad \mathbf{U}_n^T = [u_{r_n} \quad -iu_{z_n} \quad \sigma_n \quad -i\tau_n]$$

$$\mathbf{a}_n^T = [A_n \quad A_n^1 \quad iB_n \quad iB_n^1]$$

$$\mathbf{D}_n = 4 \times 4 \; layer \; matrix$$

This vector can then be propagated through all the solid layers resulting in (Tubman et al., 1984):

$$\mathbf{G}\,\mathbf{a}_n = \mathbf{U}_1(r_0) \quad (13)$$

$$where: \quad \mathbf{G} = \prod_{n=1}^{N} \mathbf{E}_n^{-1}(r_n, r_{n-1})\,\mathbf{D}_N(r_{N-1})$$

$$\mathbf{E}_n(r_n, r_{n-1}) = \mathbf{D}_n(r_n)\mathbf{D}_n^{-1}(r_{n-1})$$

Applying the boundary conditions at the fluid - solid interface yields the dispersion equation:

$$l_0 I_1(l_0 r_0)F1 + \rho_0 k^2 c^2 I_0(l_0 r_0)F2 = 0 \qquad (14)$$

$$where: \quad F1 = G_{33} G_{41} - G_{31} G_{43}$$

$$F2 = G_{13} G_{41} - G_{11} G_{43}$$

l_0, r_0, ρ_0 = *wavenumber, outer radius,* and *density of the fluid layer*

Equation (14) can be solved for the (k,c) pairs of the propagating guided modes. The Stoneley wave corresponds to $c<\alpha_0$ and the pseudo-Rayleigh to $\alpha_0 < c < \beta_N$. If β_N is less than α_0 no pseudo-Rayleigh wave will be generated and the formation is referred to as a 'slow' or 'soft' formation.

The final calculation which is needed to evaluate the integrals in equation (4) involves the amplitude constants A_n, A_n^1, B_n, B_n^1 . In order to calculate these values without imposing a source term, the A_n term is arbitrarily set equal to one (Cheng et al., 1982). The remaining constants can be determined from the propagator matrix method. The set of equations which led to the dispersion equation (14) are:

$$A_N G_{11} + B_N G_{13} = A_0^1(-l_0 I_1(l_0 r_0)) \qquad (15)$$

$$A_N G_{31} + B_N G_{33} = A_0^1(-\rho_0 k^2 c^2 I_0(l_0 r_0))$$

$$A_N G_{41} + B_N G_{43} = 0$$

Substituting $A_n = 1$ into equation (15) leads to expressions for A_0^1 and B_N :

$$A_0^1 = F2 \,/\, (l_0 I_1(l_0 r_0) G_{43}) \qquad (16)$$

$$B_N = -\frac{G_{41}}{G_{43}}$$

The constants for the intervening layers (layers 2 through N-1) can be found by equating the motion - stress vectors across the interfaces between the layers (i.e., by satisfying the boundary conditions). For example, the constants for layer N-1 can be found by solving the following equation for a_{N-1} :

$$D_{N-1}(r_{N-1}) a_{N-1} = D_N(r_{N-1}) a_N \qquad (17)$$

All the expressions needed to evaluate the partition coefficient integrals in equation (4) have now been derived. The next section applies these expressions to several

layered borehole models.

RESULTS

The calculation of partition coefficients and attenuation (Q^{-1}) from equation (4) was carried out for three models: fast formation with casing, fast formation with an invaded zone, and alow formation with casing. In all three cases, calculations were also performed for the same formation in an open hole for comparison. Casing, cement, invaded zone, and formation parameters generally follow Tubman (1984) and are given in Table 1. Frequency independent Q was assumed for all layers. All calculations for the pseudo-Rayleigh wave were carried out for the fundamental mode only.

Fast Formation - Cased borehole

Figures 2 and 4 illustrate the partition coefficients as a function of frequency for the pseudo-Rayleigh and Stoneley waves in a cased borehole with a fast formation. The casing and cement are assumed to be perfectly bonded to the formation. Layer parameters are given in Table 1. Partition coefficients for the same formation in an open hole are given in Figures 3 and 5. The higher cutoff frequency of the cased hole pseudo-Rayleigh wave is evident in Figure 2. Near the cutoff frequency the pseudo-Rayleigh wave propagates with a phase velocity approaching that of the formation shear velocity. Therefore, for both the open and cased hole geometries, the largest fraction of the wave's energy is contained in shear motion in the formation at these lower frequencies. In the open hole, as frequency increases and the phase velocity of the pseudo- Rayleigh wave approaches the fluid velocity, over 80% of the energy is propagated in the fluid (Figure 3, f>15kHz). In the cased hole the energy partitioning is more complicated. The fluid plays a much smaller role in this geometry, accounting for only 50% of the energy at 25kHz but increasing at higher frequencies (Figure 2). The casing and cement layers are most important at intermediate frequencies where 25% - 30% of the pseudo-Rayleigh wave energy is propagated as shear motion in each layer at frequencies between 17kHz and 23kHz. In both the open and cased holes there is very little energy contained in the compressional modes (less than 5%).

The Stoneley wave is predominantly propagated in the fluid layer for both the open and cased holes at all frequencies. In the open hole (Figure 5), over 80% of the energy is contained in the fluid at all frequencies. The wave is poorly coupled to the formation with only 10% - 20% of the energy propagating as shear motion and less than 5% of the energy contained in compressional motion in the formation. In the cased hole the situation is similar. At low frequencies an even greater fraction of the energy is contained in the fluid (90%) with almost no coupling to the solid layers. As the frequency increases, up to 15% - 20% of the Stoneley energy is propagated in the casing and cement layers (as shear energy) and the fluid energy drops to about 65%. There is a small fraction of compressional energy in the casing (5%) and the effect of the formation is negligible.

The resulting attenuation of the pseudo -Rayleigh and Stoneley waves is seen in Figures 6 and 7. These figures display the temporal quality factor (Q) versus frequency (increasing Q corresponds to decreasing attenuation). Due to the negligible effect of the compressional wave attenuation, only the fluid and shear wave attenuation are considered in these calculations. As expected, the pseudo-

Rayleigh wave Q increases at intermediate frequencies due to the decreased effect of the low Q fluid. The Stoneley wave Q remains essentially constant but does increase slightly at high frequencies as the fluid effect decreases. Figures 8 and 10 give the effect of the layer density on the phase velocity of the pseudo - Rayleigh and Stoneley waves for the cased hole geometry. Figures 9 and 11 give the density effects for the open hole geometry. These figures show behavior analagous to the partition coefficient results.

Fast Formation - Invaded zone

The results for a fast formation with an invaded zone are similar to those for a well bonded cased hole. Figures 12 and 13 show the partition coefficients for a 3 inch invasion zone for the pseudo-Rayleigh and Stoneley waves. Figures 14 and 15 illustrate the same quantities for a 6" invaded zone. The formation parameters are the same as in the casing example previously given. The invaded zone is assumed to have velocities 10% lower than the formation, and higher attenuation factors (Table 1). As in the cased hole example, for the pseudo-Rayleigh wave the invasion layer is most important at intermediate frequencies while the fluid effect is dominant at high frequencies and the formation shear attenuation makes the largest contribution at low frequencies. The invasion zone is much thicker than the casing and cement layers of the previous example and therefore is more dominant over a wider frequency range. As the thickness of the invasion layer is increased the formation effect shifts to lower frequencies and the invaded zone shear attenuation becomes more dominant.

The Stoneley wave partition coefficients for the invasion zone model are very similar to the open hole case; the energy is predominantly propagated in the fluid. In this case, however, the fluid energy has decreased from about 80% - 85% in the open hole to about 75% - 80% in the invasion model. At the same time, the effect of the formation has become negligible over most frequencies, while 15% - 20% of the energy is propagated as shear motion in the invaded zone. Again, compressional energy is negligible. The Stoneley wave couples with the slower invasion zone more efficiently than it does with the faster formation (Figure 3). This trend can be better illustrated by reducing the invasion zone velocities to 70% of the formation values (Figure 15a). In this case 50% of the wave's energy is propagated as shear motion in the invaded zone at frequencies greater than 10kHz and the effect of the fluid decreases with increasing frequency. The results for this 'slower' invasion zone are quite similar to the results of the next section - the slow formation.

Plots of the guided wave quality factors as functions of frequency for the invaded zone model are given in Figures 16 and 17. The pseudo-Rayleigh Q is lower compared to the open hole model at low frequencies due to the effect of the more attenuating invasion layer. At high frequencies, however, the fluid attenuation dominates in both models. The Stoneley Q increases slightly with an invasion layer due to the decreasing effect of the fluid layer and the increasing effect (better coupling) of the invasion layer. The density effects are quite similar to those given in Figures 8 and 9 and will not be included here.

Slow Formation - Cased borehole

In a soft formation ($\beta_N < \alpha_0$) no pseudo-Rayleigh wave is generated. The partition coefficients for a soft formation in an open hole are given in Figure 18. In this case the Stoneley wave is well coupled to the formation and the formation shear

attenuation is dominant at high frequencies while the fluid is more important at low frequencies. The addition of casing and cement layers (Figure 19) seems to accentuate the behavior seen in the open hole. The casing and cement layers carry little or no energy, and there is negligible compressional energy propagated in the formation. The Stoneley wave Q for the open and cased hole geometry is shown in Figure 20. The trend of the two curves is similar; however, the cased hole curve has a much sharper inflection and quickly reaches the value of the formation shear Q as frequency increases. The density of the formation affects the phase velocity more strongly at high frequencies in an open hole (Figure 21). The density effects are similar for a cased hole and need not be illustrated.

DISCUSSION AND CONCLUSIONS

The results of the previous section indicate that the partition coefficient values are quite variable with frequency. The effect of the casing or invaded layer is restricted to a limited frequency range which is related to the thickness of the layer. The curves for the invasion layer of varying thickness (Figures 12 and 14) illustrate this very clearly. For pseudo-Rayleigh waves the frequency dependence is due to the depth of penetration of the spectral components of the guided wave. The range of depth of penetration can be illustrated by the radial displacements as a function of radial distance for a high (39.961 kHz) and low (12.643 kHz) frequency component of the pseudo-Rayleigh wave in a cased hole in Figures 22 and 23. The low frequencies see further into the medium and hence a larger fraction of the energy is propagated in the formation. High frequencies on the other hand have a very shallow penetration depth and most energy is carried in the fluid. The attenuation of the guided waves exhibits a similar frequency dependence. The addition of casing and cement layers reduces the attenuation of the pseudo-Rayleigh wave over the intermediate frequencies due to the decreasing effect of the highly attenuating fluid. The presence of an invasion layer increases the attenuation of the pseudo-Rayleigh wave due to the more attenuating invaded zone. In both cases, however, Q_{pr}^{-1} approaches Q_{β}^{-1} of the formation at low frequencies and Q_{α}^{-1} of the fluid at high frequencies. These results explain the amplitude variations of the synthetic FWALs in invaded boreholes generated by Tubman (1984). The amplitude variations in the cased hole synthetics, however, are mostly dominated by the reduction in the radius of the fluid layer.

The Stoneley wave partition coefficients behave somewhat differently than the pseudo-Rayleigh wave coefficients. In an open hole with a fast formation, the fluid layer is dominant at all frequencies and the wave is weakly coupled to the formation. The addition of casing reduces the fluid effect somewhat at higher frequencies and the wave has some coupling with the casing and cement, although the fluid is completely dominant at low frequencies. If a slower invasion layer is added, the wave is more strongly coupled to the solid invasion layer. As the invasion layer or formation becomes slower, the Stoneley wave becomes more efficiently coupled to the solid. This is especially true for a 'slow' formation where most energy is propagated as shear motion in the formation at higher frequencies. The addition of casing and cement layers to such a 'slow' formation model does not alter this overall energy partitioning, although it does seem to shift the frequency range over which the fluid and formation layers dominate (Figures 18, 19). This variation in Stoneley wave coupling between the solid and fluid layers can be illustrated by examining plots of the radial displacement. Figure 24 shows the radial displacement for a Stoneley wave component (2647 Hz) in an open hole with a fast formation. Figure 25

shows the same quantity for an open hole in a slow formation (2668 Hz). The higher amplitude and deeper penetration of the wave in the slow formation illustrates the more efficient coupling of the wave as the velocity of the solid layer decreases. A similar effect can be seen for a fast and slow formation in the presence of casing (Figures 26 and 27). Figure 26 shows the radial displacement for the Stoneley wave in a well bonded cased hole with a fast formation (1070 Hz), while Figure 27 shows the same quantity for a slow formation in a cased hole (1073 Hz). It should be noted that in all these cases (Figures 24 through 27) the axial displacement in the fluid is several orders of magnitude greater than the radial displacement, and the axial displacement in the solid layers is much less (by a factor of 10 to 100) than the axial displacement in the fluid.

ACKNOWLEDGEMENTS

D.R. Burns was partially supported by a Phillips Petroleum Fellowship. The work is supported by the Full Waveform Acoustic Logging Consortium at M.I.T.

REFERENCES

Aki, K. and Richards, P., 1980, Quantitative seismology theory and methods, v.I : San Francisco, W. H. Freeman and Co.

Anderson, D.L. and Archambeau, C.B., 1964, The anelasticity of the earth: J. Geophys. Res., v.69, p.2071-2084.

Baker, L.J., 1984, The effect of the invaded zone on full wavetrain acoustic logging: Geophysics, v.49, p.796-809.

Chan, A.K. and Tsang, L., 1983, Propagation of acoustic waves in a fluid-filled borehole surrounded by a concentrically layered transversely isotropic formation: J. Acoust. Soc. of Am., v.74, p.1605-1616.

Cheng, C.H. and Toksöz, M.N., 1981, Elastic wave propagation in a fluid- filled borehole and synthetic acoustic logs: Geophysics, v.46, p.1042-1053.

Cheng, C.H., Toksöz, M.N. and Willis, M.E., 1982, Determination of in-situ attenuation from full waveform acoustic logs: J. Geophys. Res., v.87, p.5477-5484.

Paillet, F.L. and White, J.E., 1982, Acoustic modes of propagation in the borehole and their relationship to rock properties: Geophysics, v.47, p.1215-1228.

Schoenberg, M., Marzetta, T., Aron, J., and Porter, R., 1981, Space-time dependence of acoustic waves in a borehole: J. Acoust. Soc. of Am., v.70, p.1496- 1507.

Tsang, L. and Rader, D., 1979, Numerical evaluation of the transient acoustic waveform due to a point source in a fluid-filled borehole: Geophysics, v.44, p.1706-1720.

Tubman, K.M., 1984, Synthetic full waveform acoustic logs in radially layered boreholes: Ph.D. thesis, MIT, Cambridge,MA.

Tubman, K.M., Cheng, C.H., and Toksöz, M.N., 1984, Synthetic full waveform acoustic logs in cased boreholes: Geophysics, v.49, p.1051-1059.

Layer	α		β		$\rho(gm/cc)$	Q_α	Q_β
	ft/sec	m/sec	ft/sec	m/sec			
fluid	5500	1676	0	0	1.2	20	0
casing	20000	6096	11000	3353	7.5	1000	1000
cement	9260	2822	5670	1728	1.92	40	30
fast fm	16000	4877	8530	2600	2.16	60	60
inv zone	14400	4389	7677	2340	2.36	40	40
slow fm	9022	2750	3940	1200	2.1	50	50

table 1

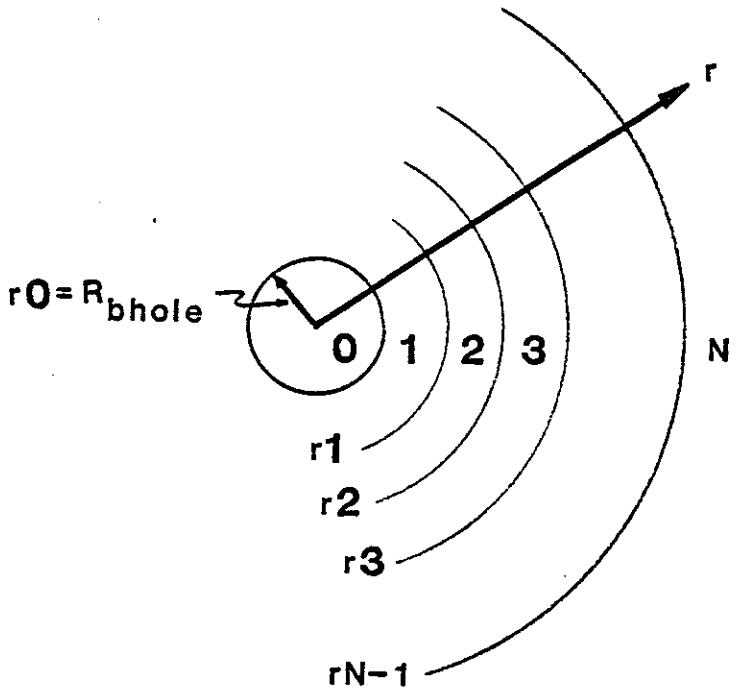

Figure 1: Geometry of a radially layered borehole.

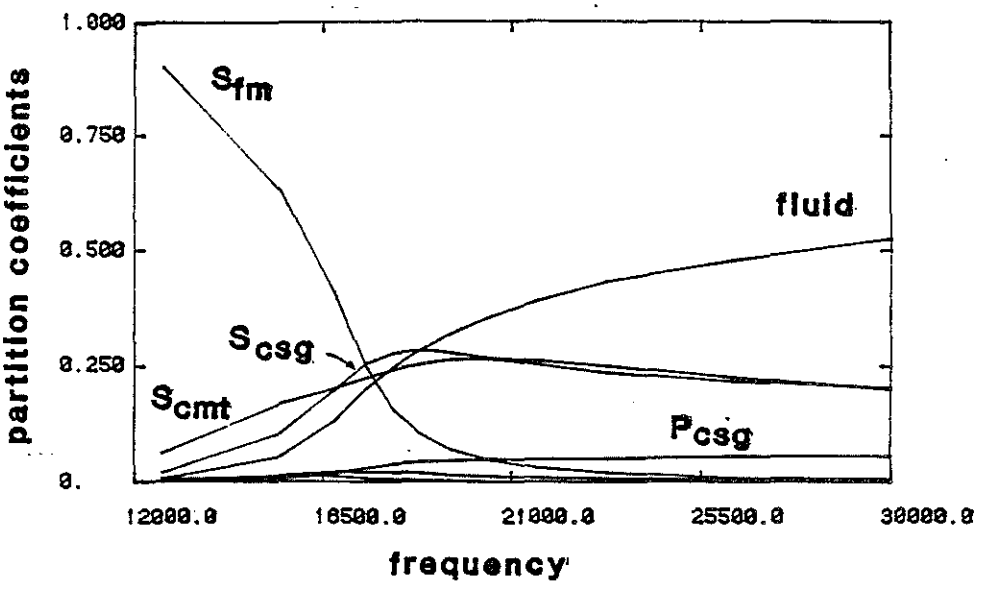

Figure 2: Partition coefficients for the pseudo-Rayleigh wave in a cased borehole with a fast formation. S and P refer to shear and compressional motion, csg indicates the casing layer, cmt indicates the cement layer, and fm indicates the formation. (these abbreviations will be used in the following figures as well)

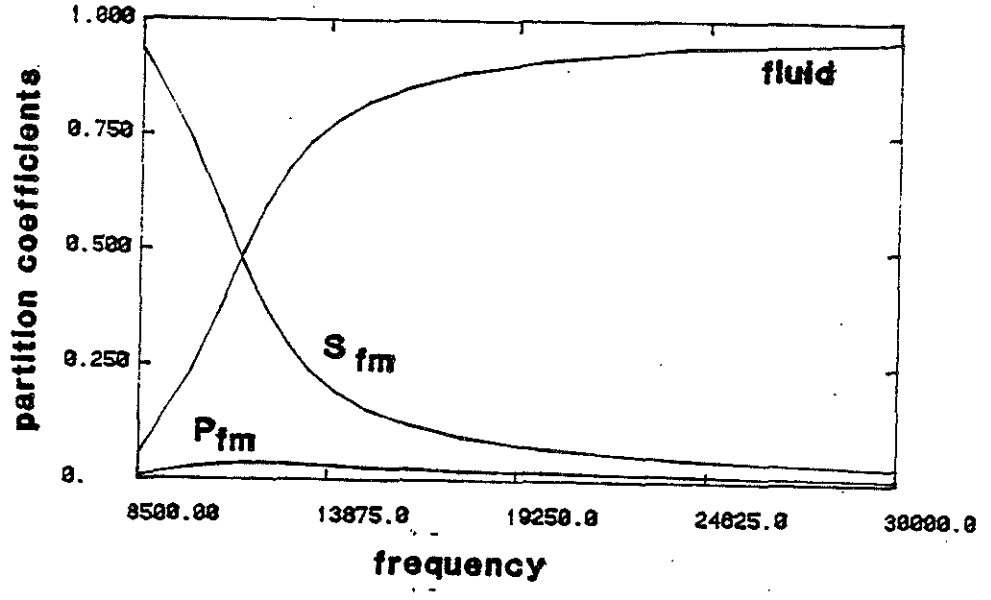

Figure 3: Partition coefficients for the pseudo-Rayleigh wave in an open borehole with a fast formation.

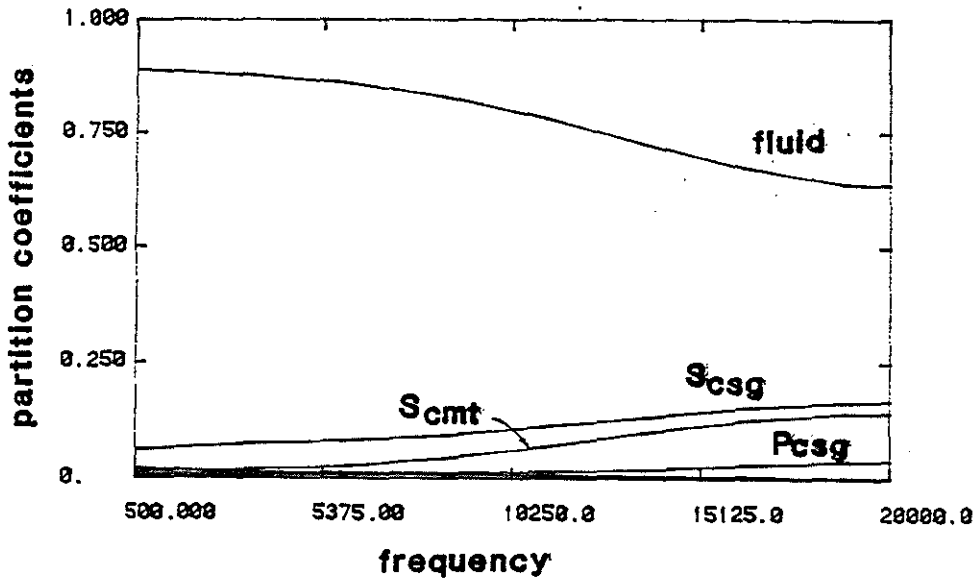

Figure 4: Partition coefficients for the Stoneley wave in a cased borehole with a fast formation.

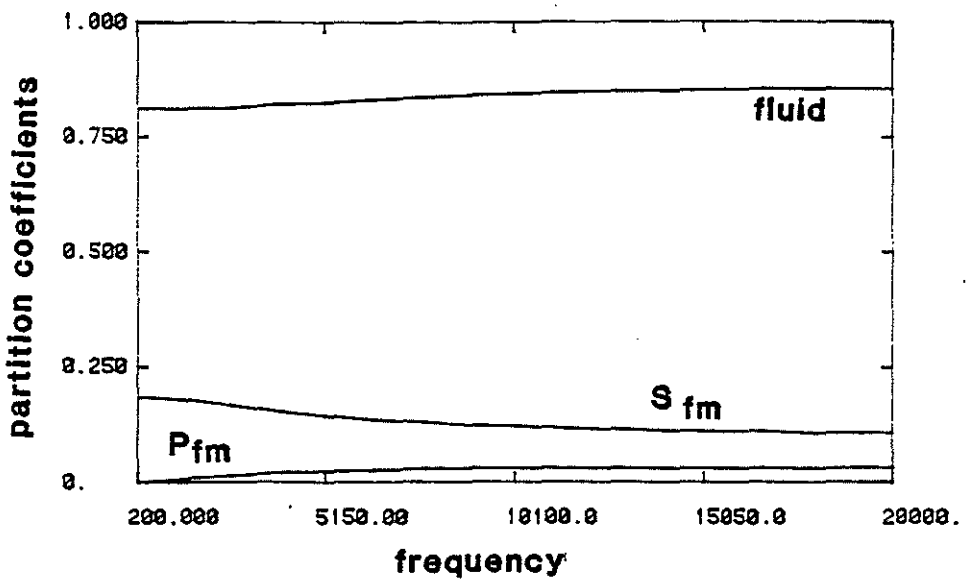

Figure 5: Partition coefficients for the Stoneley wave in an open borehole with a fast formation.

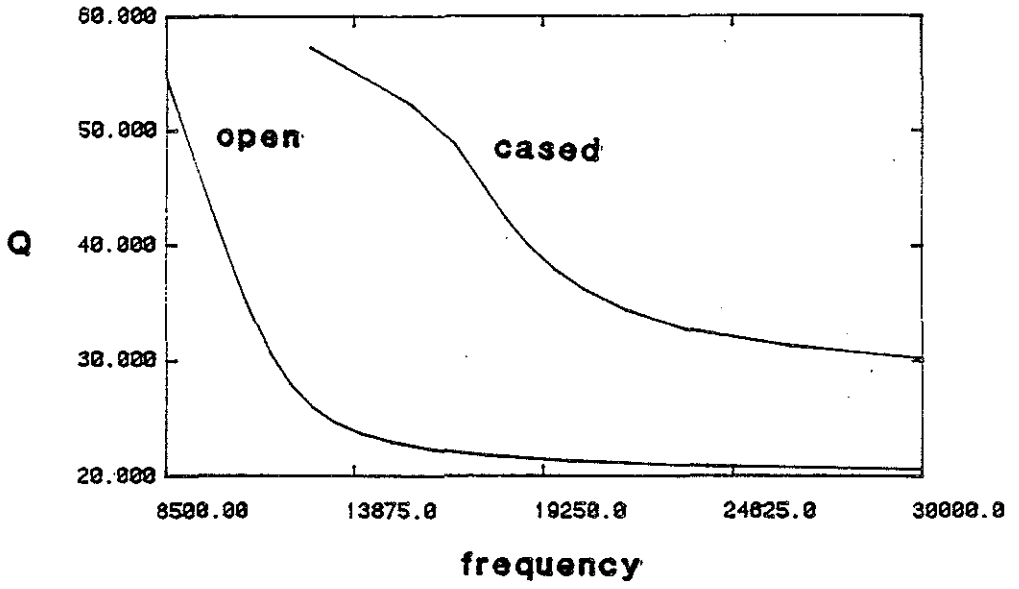

Figure 6: Pseudo-Rayleigh wave quality factor for open and cased hole geometries.

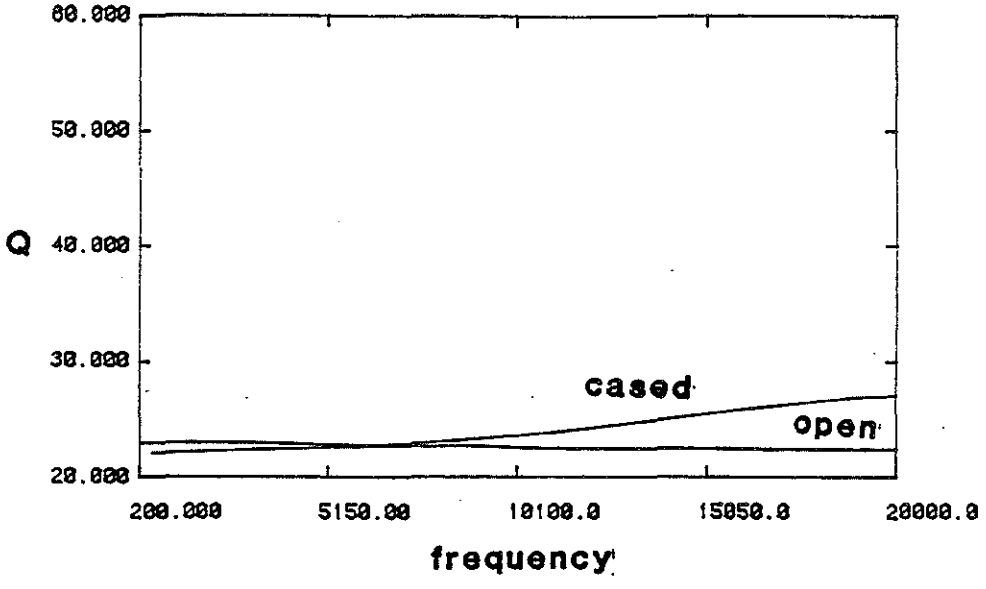

Figure 7: Stoneley wave quality factor for open and cased hole geometries.

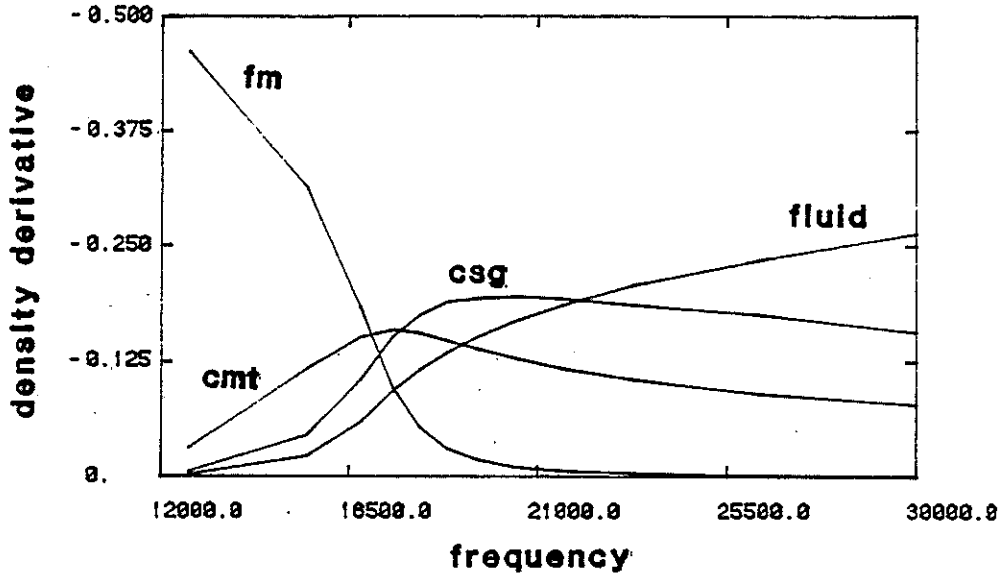

Figure 8: Density derivatives for the pseudo-Rayleigh wave in a cased borehole with a fast formation

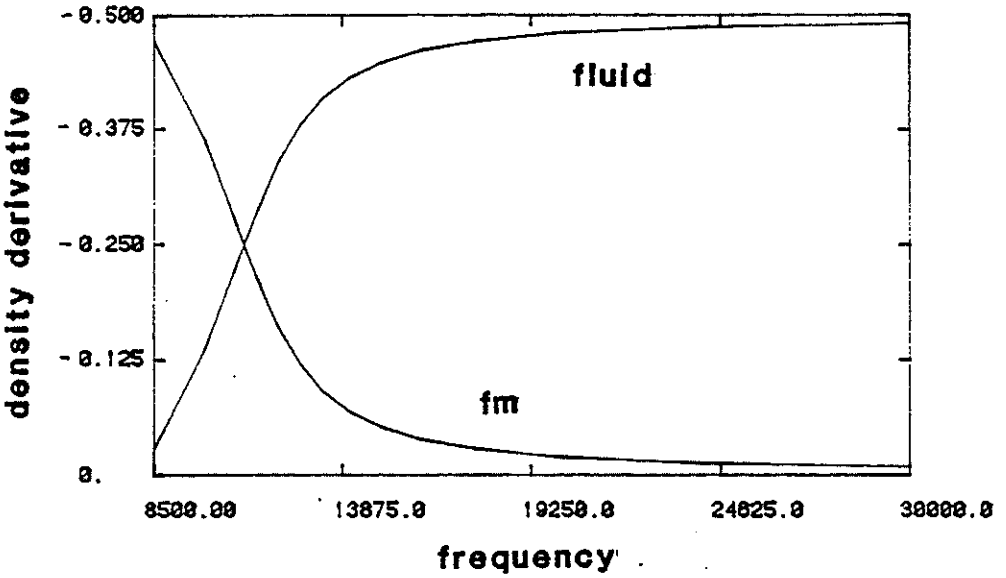

Figure 9: Density derivatives for the pseudo-Rayleigh wave in an open borehole with a fast formation.

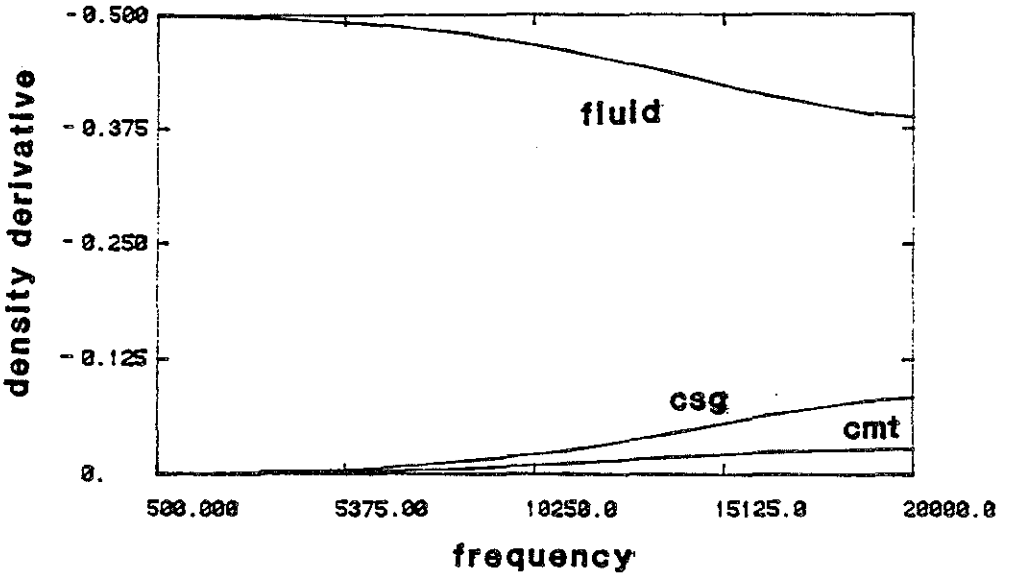

Figure 10: Density derivatives for the Stoneley wave in a cased borehole with a fast formation.

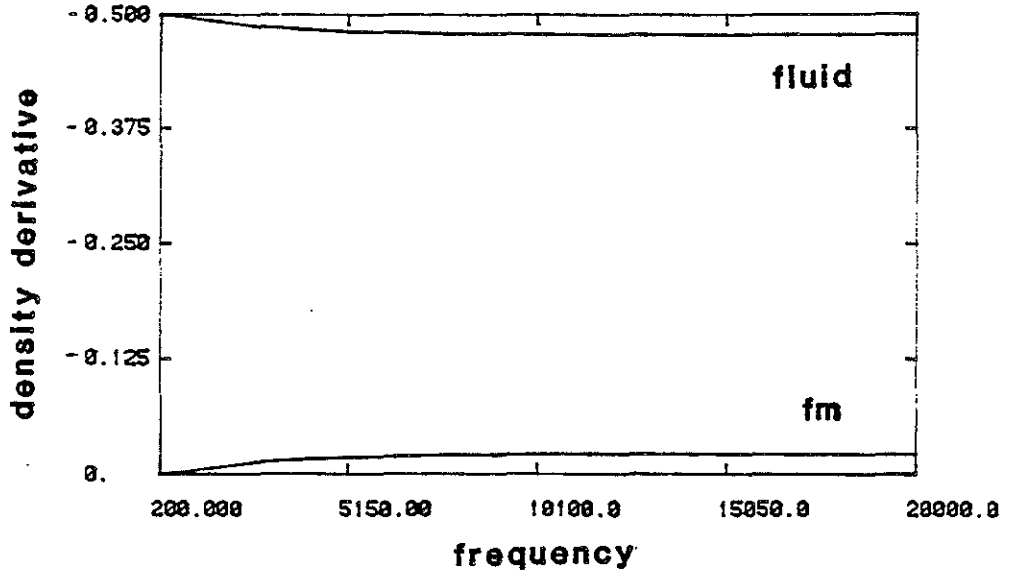

Figure 11: Density derivatives for the Stoneley wave in an open borehole with a fast formation.

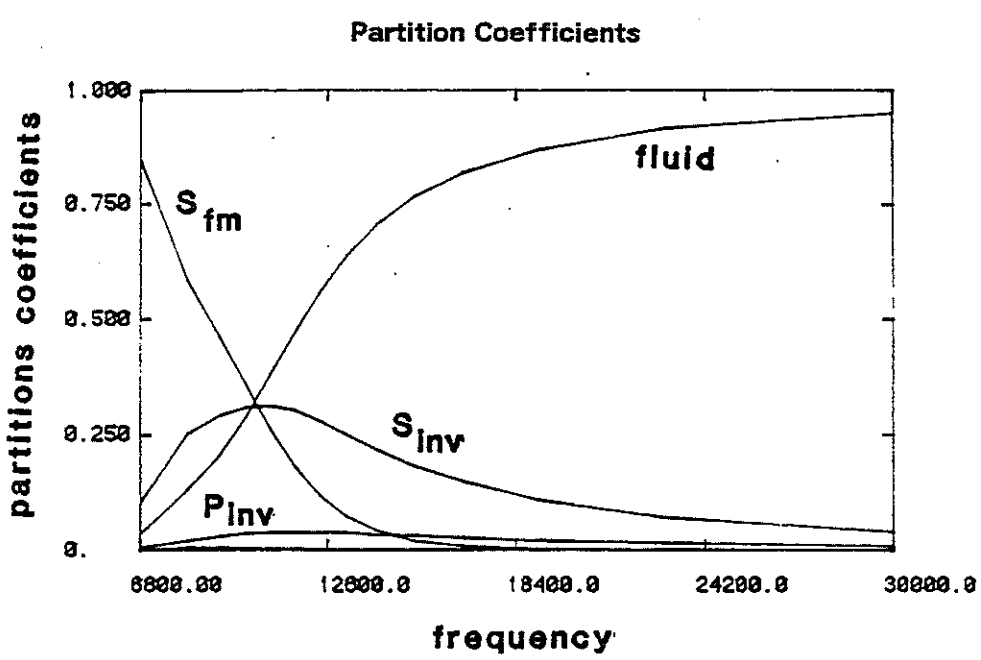

Figure 12: Partition coefficients for the pseudo-Rayleigh wave in a borehole with a 3" invasion zone and a fast formation. Inv indicates the invasion zone layer. (this abbreviation will be used in the following figures as well)

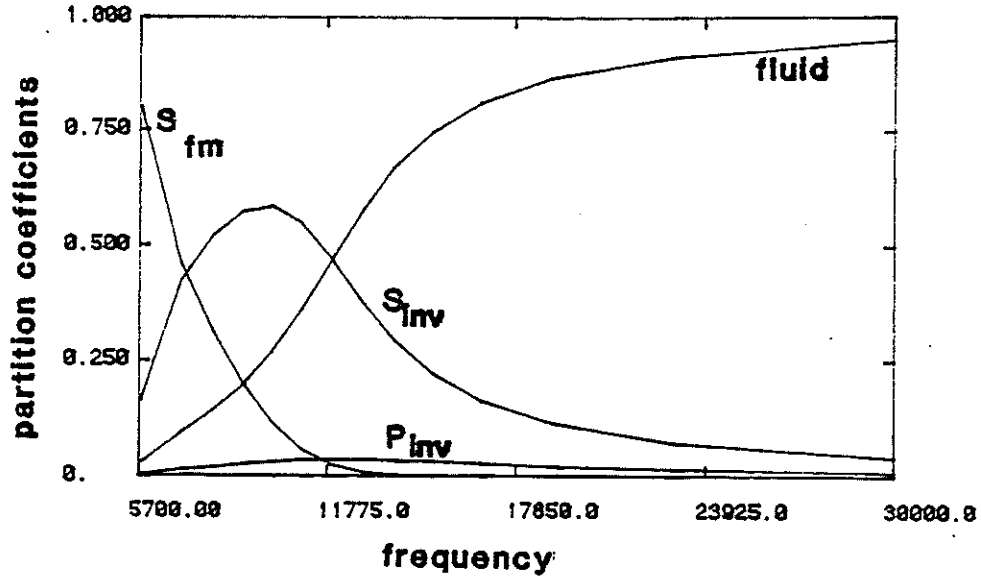

Figure 13: Partition coefficients for the pseudo-Rayleigh wave in a borehole with a 6" invasion zone and a fast formation.

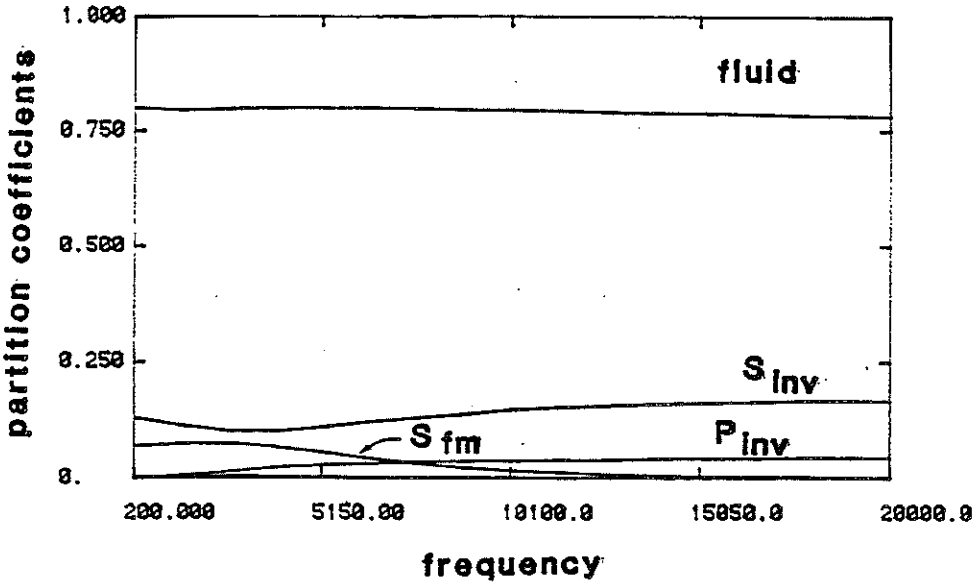

Figure 14: Partition coefficients for the Stoneley wave in a borehole with a 3" invasion zone and a fast formation.

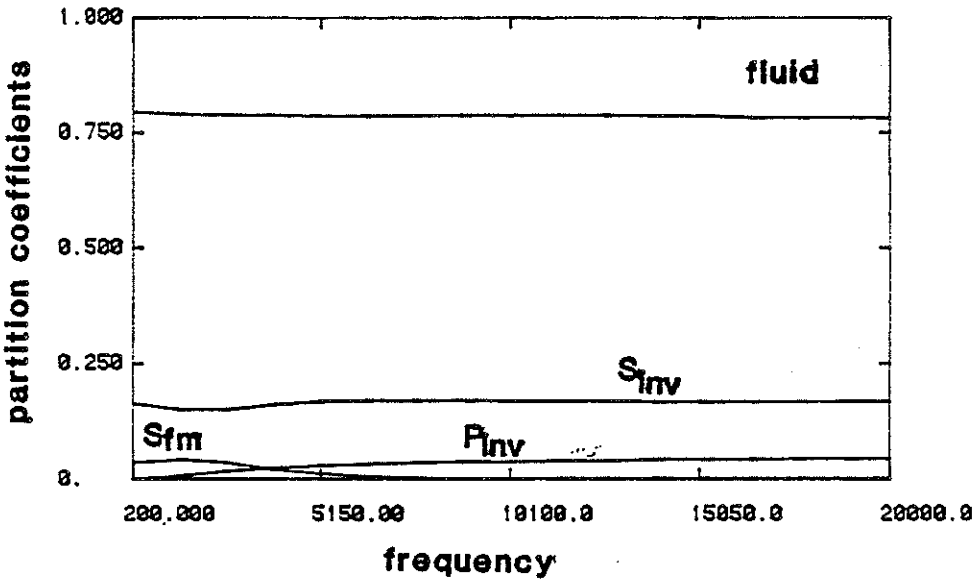

Figure 15: Partition coefficients for the Stoneley wave in a borehole with a 6" invasion zone and a fast formation.

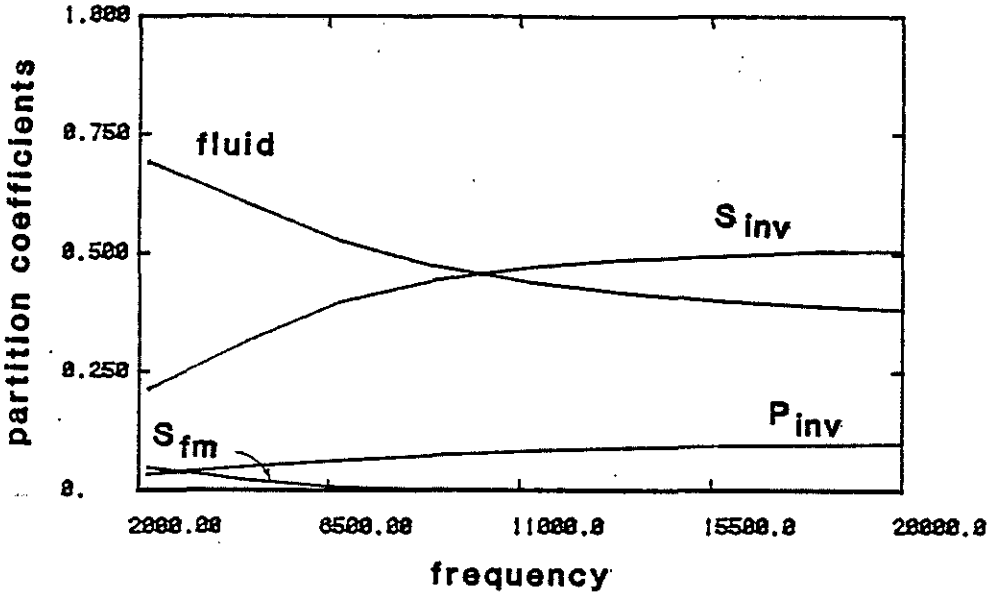

Figure 15a: Partition coefficients for the Stoneley wave in a borehole with a 6" invasion zone and a fast formation. The invasion zone in this case has velocities 30% lower than the formation velocities (compared to 10% lower in the previous figures).

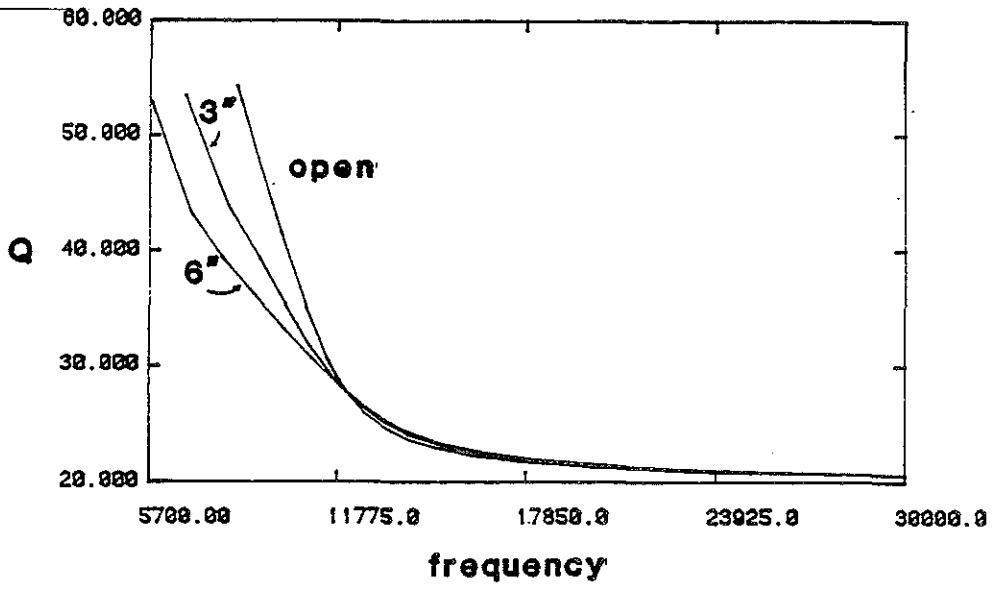

Figure 16: Pseudo-Rayleigh wave quality factor for open and invaded zone borehole models.

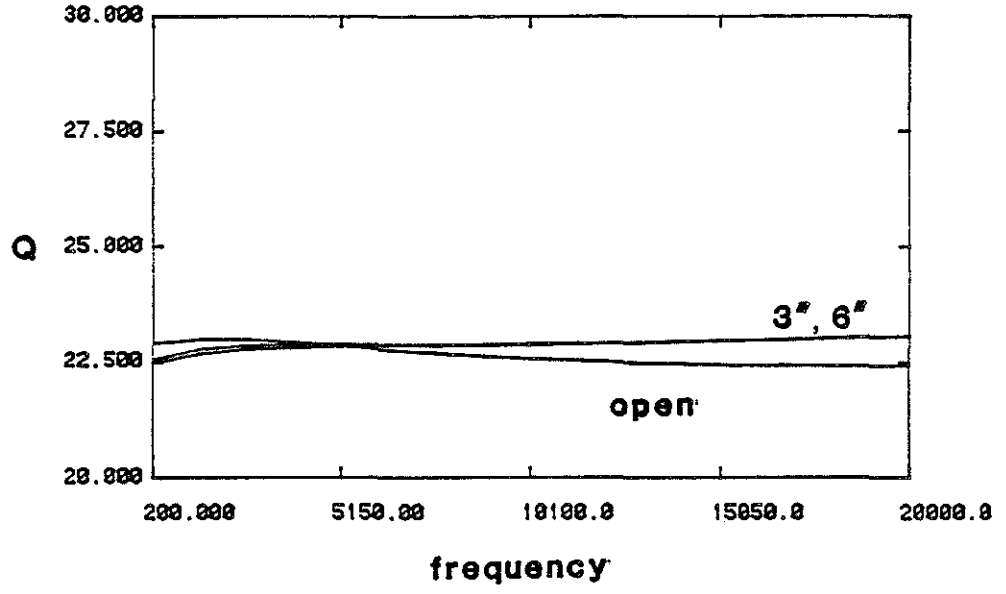

Figure 17: Stoneley wave quality factor for open and invaded zone borehole models (fast formation).

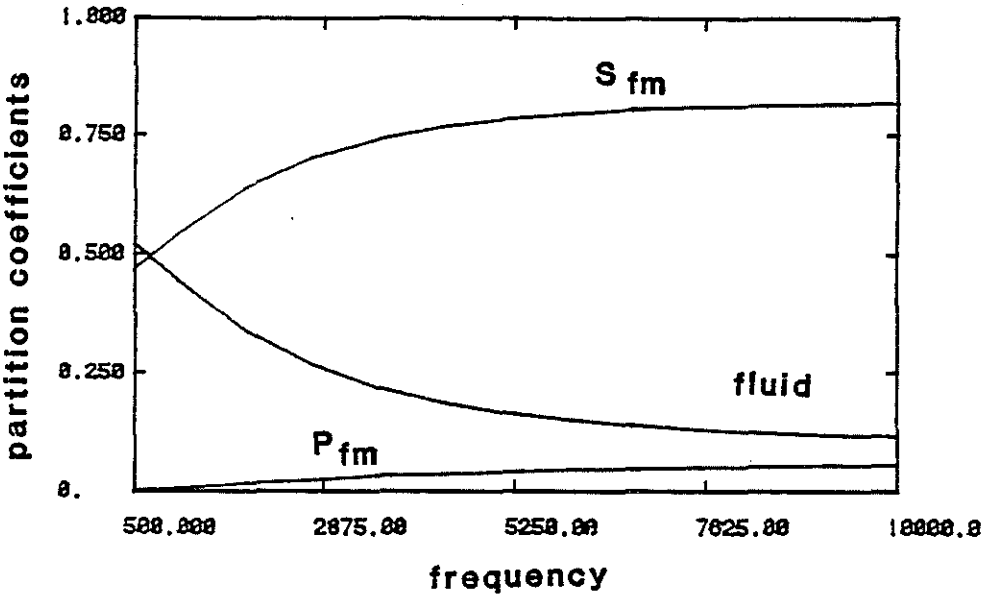

Figure 18: Partition coefficients for the Stoneley wave in an open borehole with a slow formation.

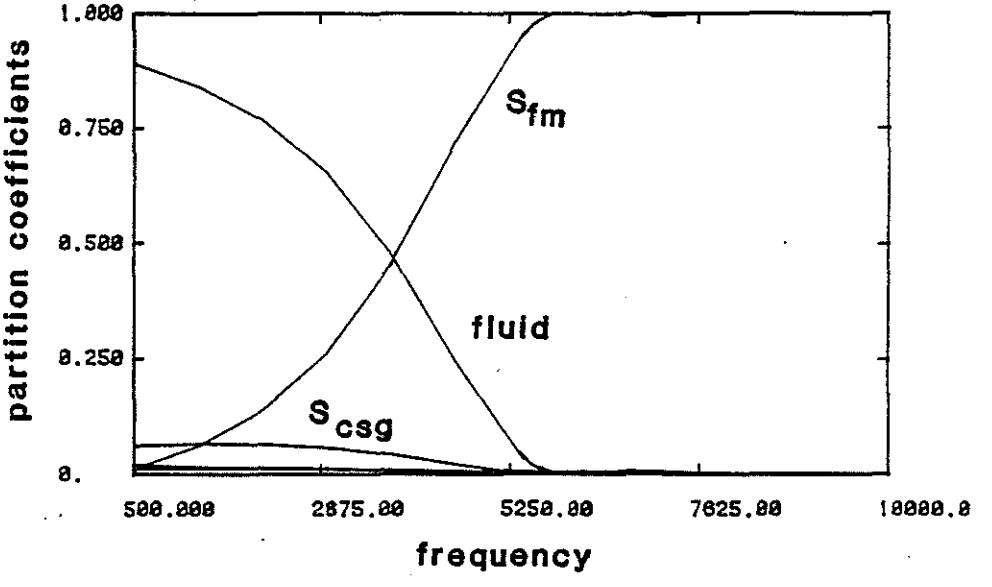

Figure 19: Partition coefficients for the Stoneley wave in a cased borehole with a slow formation.

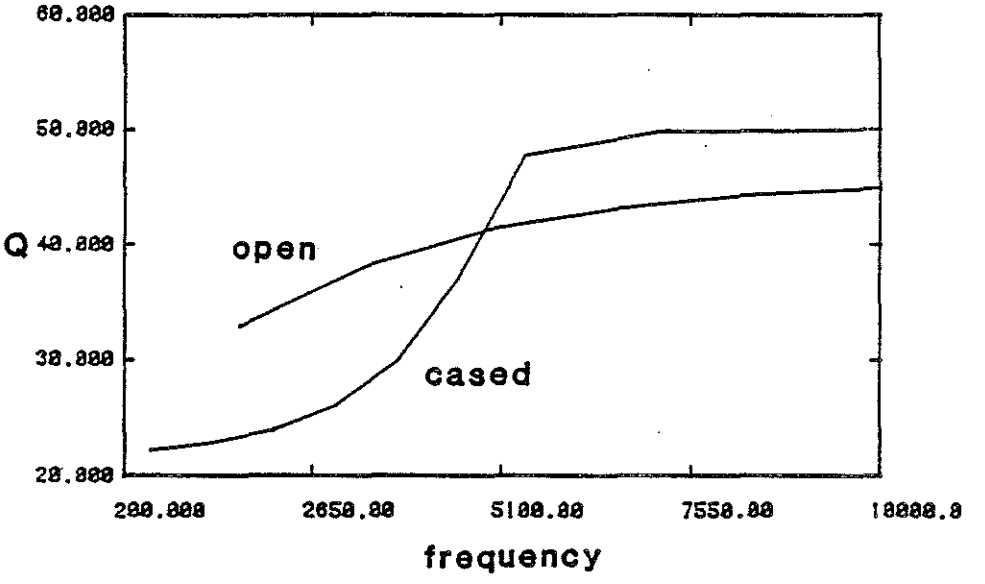

Figure 20: Stoneley wave quality factor for the open and cased borehole models with a slow formation.

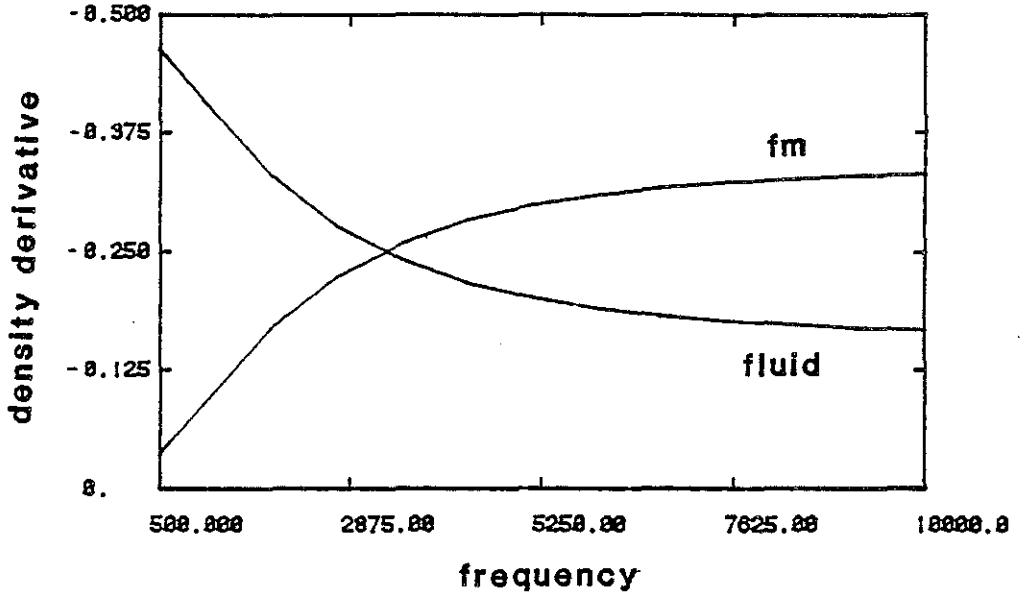

Figure 21: Density derivatives for the Stoneley wave in an open borehole with a slow formation.

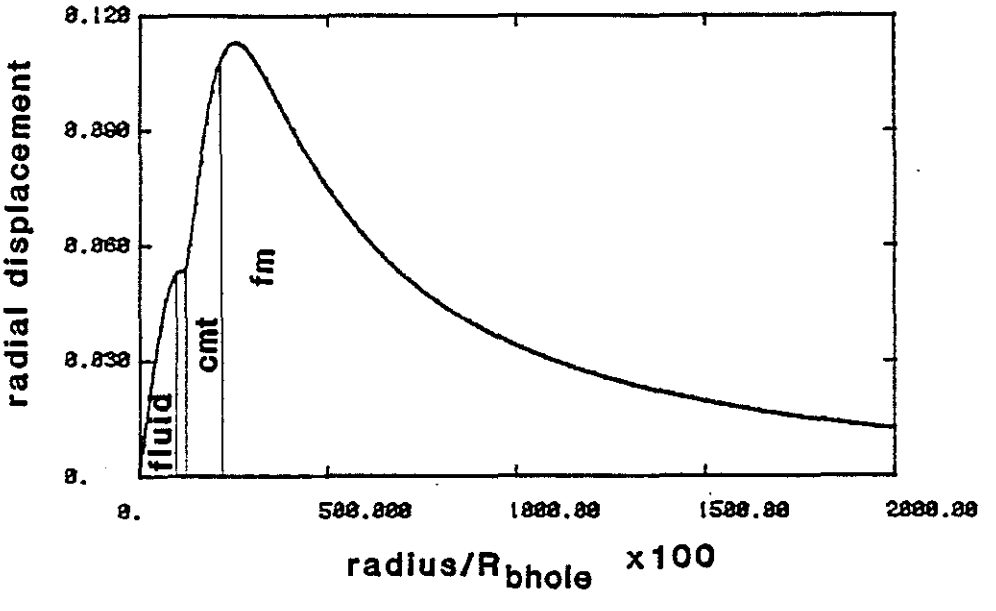

Figure 22: Radial displacement of a low frequency component (12643 Hz) of the pseudo-Rayleigh wave in a cased borehole.

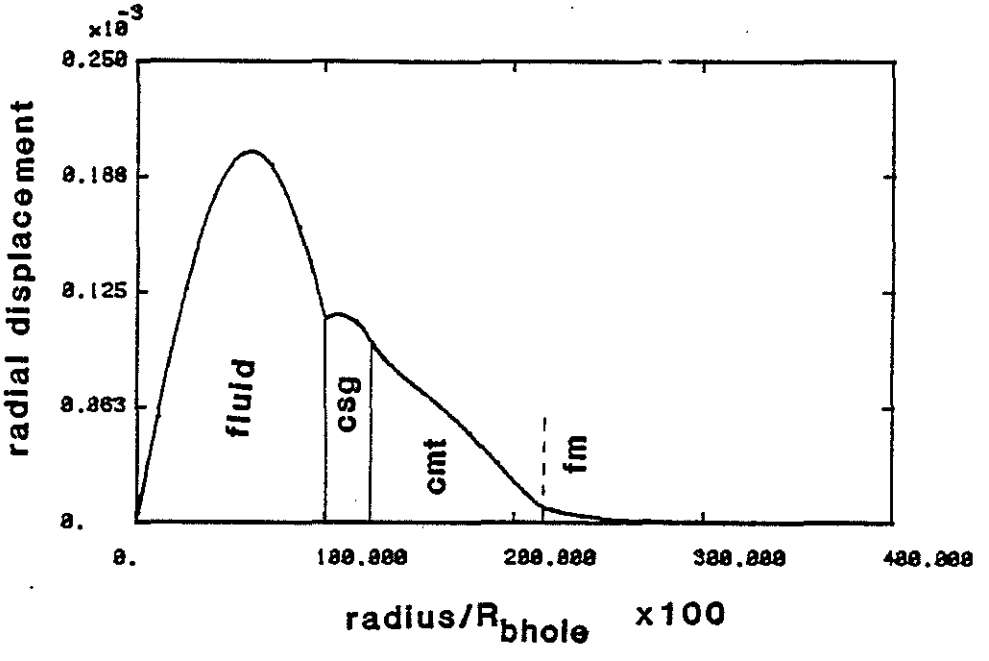

Figure 23: Radial displacement of a high frequency component (39961 Hz) of the pseuso-Rayleigh wave in a cased borehole.

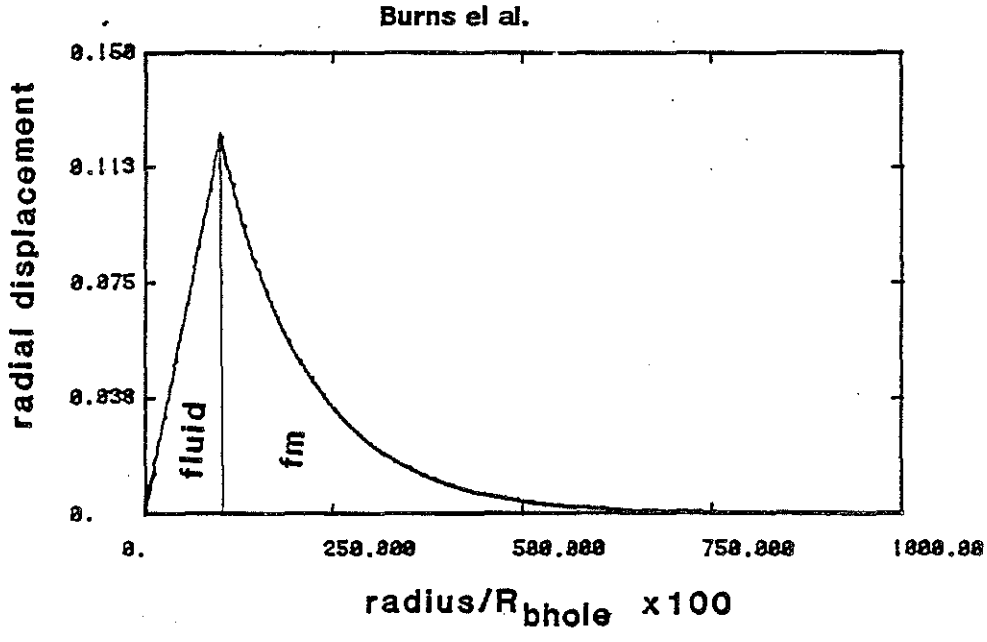

Figure 24: Radial displacement of a component (2647 Hz) of the Stoneley wave in an open borehole with a fast formation.

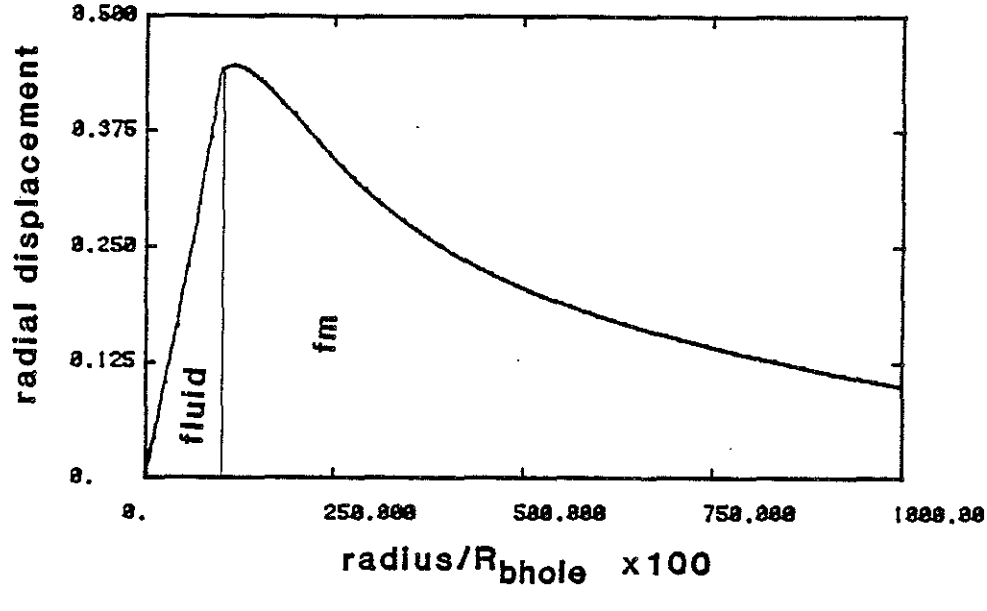

Figure 25: Radial displacement of a component (2668 Hz) of the Stoneley wave in an open borehole with a slow formation.

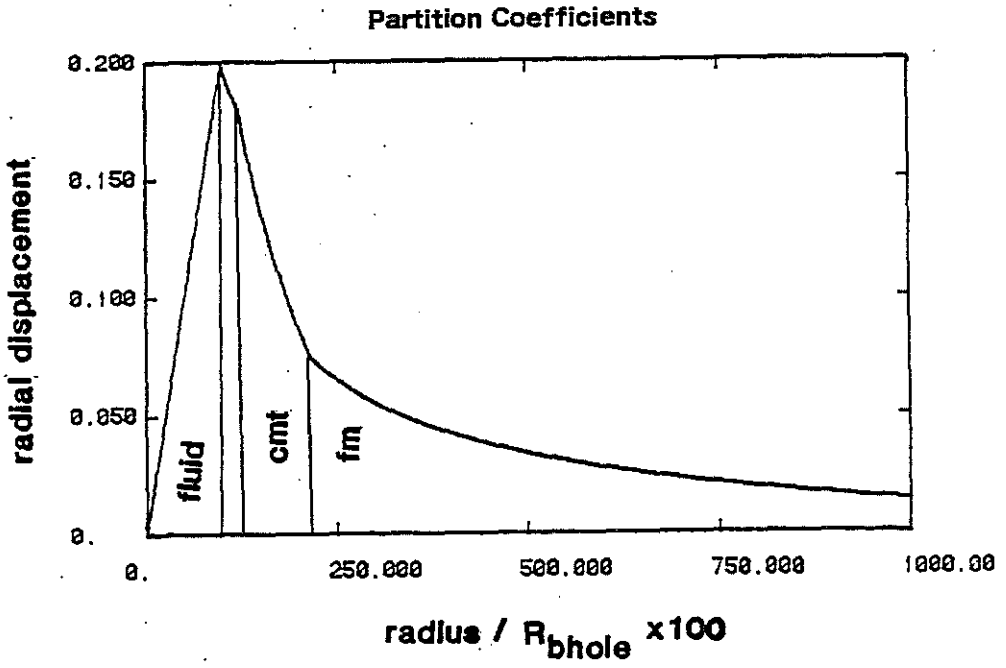

Figure 26: Radial displacement of a component (1070 Hz) of the Stoneley wave in a cased borehole with a fast formation.

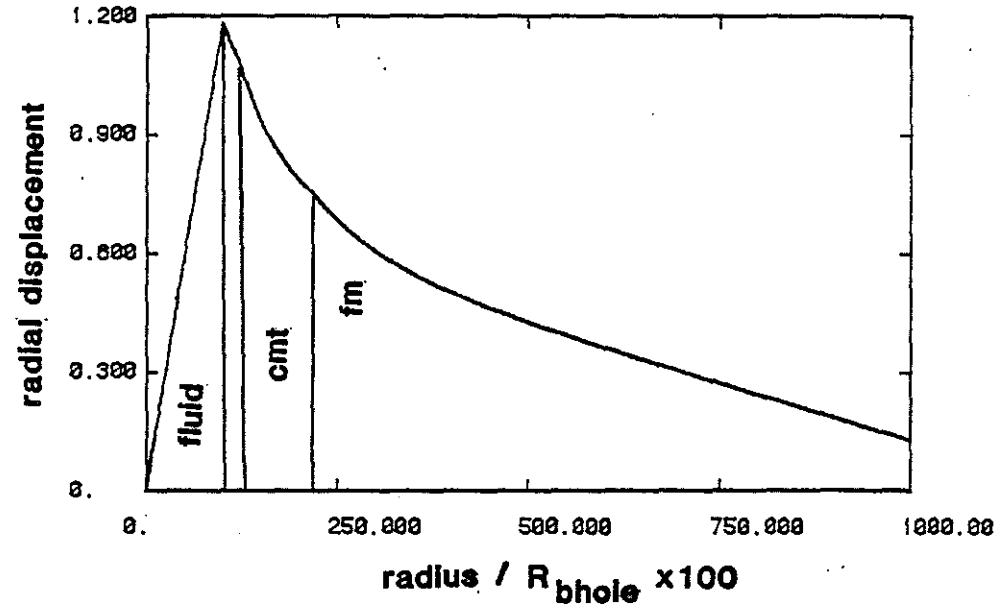

Figure 27: Radial displacement of a component (1073 Hz) of the Stoneley wave in a cased borehole with a slow formation.